

## Phase Transitions and Universal Dynamics in Confined Films

Peter A. Thompson and Gary S. Grest

*Corporate Research Science Laboratories, Exxon Research and Engineering Company, Annandale, New Jersey 08801*

Mark O. Robbins

*Department of Physics and Astronomy, Johns Hopkins University, Baltimore, Maryland 21218*

(Received 31 January 1992)

We describe molecular dynamics simulations of fluid films confined between two solid walls. The films consist of spherical molecules, or flexible linear chains with up to twenty monomers. When the wall separation is only a few molecular diameters, crystalline or glassy order is induced across the film. The onset of the glassy phase is characterized by rapidly increasing relaxation times. These manifest themselves through changes in the diffusion constant and in the response to shear. The viscosity exhibits the same power-law scaling with shear rate that was observed in recent experiments. Our study suggests that this response is a universal property of lubricants near a glass transition.

PACS numbers: 68.15.+e, 62.15.+i, 64.70.Pf, 81.40.Pq

When fluids are confined between solid walls separated by only a few molecular diameters, their structural and dynamical properties are drastically altered [1–5]. Experiments reveal wall-induced layering of fluid films at wall separations of up to  $\sim 20$  molecular diameters [1,2]. At smaller separations, the viscosity increases by several orders of magnitude [3,4]. In many cases the film develops a yield stress, indicating a transition to a solidlike state [3–5]. When sheared slowly, these solidlike films may exhibit oscillatory stick-slip motion [5].

Computer simulations of films with simple spherical molecules have played a pivotal role in understanding the origin of these phenomena [6–10]. In particular, they reveal substantial in-plane ordering of molecules [7–9] in addition to the layering noted above [6,7]. This in-plane order plays an essential role in transmitting shear stress [7]. The entire film may crystallize when the wall separation is less than  $\sim 5$ –6 molecular spacings, leading to a finite yield stress [8,9]. Stresses greater than this value destroy crystalline order. Stick-slip motion involves periodic shear melting and recrystallization of the film [9].

In spite of their successes, simulations with spherical molecules have been unable to reproduce several key features of the experimental data. For example, the calculated relaxation times and viscosities remain near bulk fluid values until the film crystallizes. In experiments, both quantities may increase by many orders of magnitude before a yield stress is observed [3–5]. Moreover, recent work [11] indicates that there may be a power-law distribution of relaxation times with a universal exponent. In sufficiently thin films and at high shear rates, the measured viscosity decreases with shear rate as  $\dot{\gamma}^{-1/2}$ —independent of the molecular composition of the film.

In this paper, we examine whether these phenomena can be attributed to *intramolecular* dynamics. We describe molecular dynamics simulations of films composed of freely jointed, linear-chain molecules confined between

two solid walls. As observed in studies of spherical molecules [7–10], confinement decreases the entropy of these films and shifts the bulk phase transitions to higher temperatures and lower pressures. However, films of chain molecules undergo a glass transition instead of crystallizing. Near the glass transition there are dramatic increases in the viscosity and relaxation times. Moreover, the films exhibit the same power-law viscous response that was observed in experiments [11]. The robustness of the power law despite changes in the chain length and wall-chain interactions suggests that it is a generic feature of glassy films under shear. Other properties exhibit less universality. Among the interesting effects are localization of strain to the wall-chain interface and decreases in the apparent viscosity with decreasing wall separation.

The simulations were performed in a planar, Couette geometry that closely resembles the experimental systems [3–5]. A thin film of fluid molecules was confined between two solid walls with periodic boundary conditions in the plane of the walls. Each wall consisted of  $2N_w$  atoms forming two (111) planes of an fcc lattice. The wall atoms were coupled to lattice sites via stiff springs [7]. Several values of the nearest-neighbor spacing  $d$  were used to explore the effect of commensurability between wall and fluid molecules.

A well-studied bead-spring model was used for the chain molecules [12]. Monomers separated by a distance  $r$  interacted through a purely repulsive, truncated Lennard-Jones (LJ) potential,

$$V(r) = 4\epsilon[(\sigma/r)^{12} - (\sigma/r)^6 + (\sigma/r_c)^6 - (\sigma/r_c)^{12}]. \quad (1)$$

Here,  $\epsilon$  and  $\sigma$  are characteristic energy and length scales and the potential is zero for  $r > r_c = 2^{1/6}\sigma$ . Adjacent monomers along each chain of length  $n$  were also coupled through a strongly attractive potential,

$$V^{ch}(r) = -kR_0^2 \ln[1 - (r/R_0)^2], \quad r < R_0, \quad (2)$$

where  $R_0=1.5\sigma$  and  $k=15\epsilon/\sigma^2$ . Previous studies have shown that this potential prevents chain crossings and yields realistic dynamics for polymer melts [12]. At the densities considered in our study, the mean bond length was  $\sim 0.96\sigma$ . The wall-monomer interaction was also modeled with a truncated LJ potential [Eq. (1)], with parameters  $\epsilon^{wf}$ ,  $\sigma^{wf}$ , and  $r_c^{wf}$ .

To mimic experiments [3–5], the simulations were done with a constant pressure  $P_\perp$  applied between the walls. The dynamics of the wall separation  $h$  were modeled using a generalization of Andersen's extended system method [13]. A constant temperature,  $T=1.1\epsilon/k_B$ , was maintained by coupling the motion of the wall molecules to a thermal reservoir [12]. The equations of motion were integrated using a fifth-order predictor-corrector algorithm with time step  $\Delta t=0.005\tau$ , where  $\tau=(m\sigma^2/\epsilon)^{1/2}$ .

Layering produces oscillations in  $P_\perp$  with  $h$  [1,14]. The walls are pulled together when  $h$  is just larger than an integral number of layers and repelled when  $h$  is smaller. The number of fluid molecules  $N_f$  is nearly constant over a wide range of  $P_\perp$  and then decreases suddenly as a layer is squeezed out [14]. Recent simulations show that allowing  $N_f$  to vary does not produce significant changes in the dynamics of films of spherical molecules [10]. We thus fixed  $N_f=m_l N_l$ , corresponding to  $m_l$  layers of  $N_l$  molecules. For the results in Figs. 1–3,  $N_l=N_w=144$ .

We start by considering the effect of confinement on equilibrium properties. As noted above, an isolated solid surface induces both normal [6,7] and in-plane [7] order in adjacent fluids. This ordering is greatly enhanced as two surfaces approach. In-plane ordering has received less attention than layering, but is more important in determining friction and flow boundary conditions [7,15]. It determines the effective capillary size of pores [7], and the dissipation during spreading on solids [15]. One measure of the amount of in-plane order is the Debye-Waller factor,  $S_{\max}/S(0)$ , where  $S_{\max}$  is the largest peak height in the two-dimensional structure factor of a layer adjacent to the solid wall. The limiting values of  $S_{\max}/S(0)$  are 1 and 0, corresponding to a crystal at  $T=0$  and a fluid decoupled from the wall.

Figure 1 shows the dependence of  $h$ ,  $S_{\max}/S(0)$ , and the molecular diffusion constant parallel to the walls,  $D$ , on  $P_\perp$  and chain length for  $m_l=2$ . As expected, the film thickness decreases slightly with increasing  $P_\perp$ . At the same time, the degree of layering and in-plane order increases, and the diffusion constant decreases. The major difference between spherical and chain molecules is in the form of these changes. There is a sudden drop in  $D$  and a transition to an fcc structure with  $S_{\max}/S(0) > 0.6$  in monomer films [16]. The transition pressure  $P_\perp \approx 7\epsilon\sigma^{-3}$  is substantially lower than the bulk value of  $P \approx 12\epsilon\sigma^{-3}$ . In contrast, films of chain molecules remain highly disordered. The steady drop in  $D$  relative to bulk values indi-

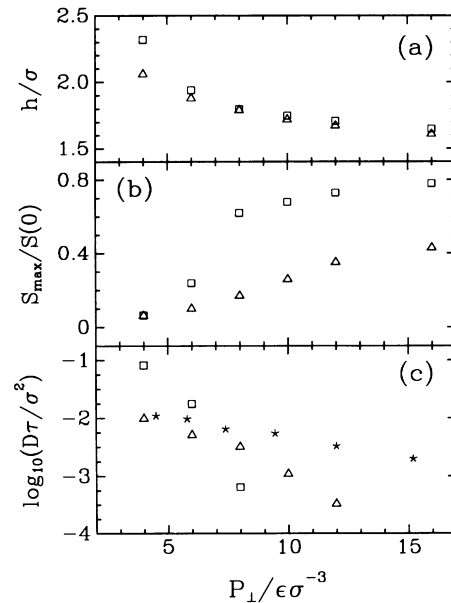


FIG. 1. Variation of (a) wall separation, (b) Debye-Waller factor, and (c) molecular diffusion constant with  $P_\perp$  in static two-layer films with  $\epsilon^{wf}=\epsilon$ ,  $r_c^{wf}=2^{1/6}\sigma$ , and  $d=1.20\sigma$ . Squares and triangles indicate films with  $n=1$  and  $n=6$ , respectively. Stars indicate the bulk diffusion for  $n=6$ .

cates the onset of a glassy phase at a pressure below the bulk transition pressure. Thus confinement produces a marked shift in the bulk transition pressures of both types of molecules. The magnitude of the shift depends on  $m_l$ , the strength of the wall-fluid interaction, and the commensurability between wall and fluid. The nature of the transition may also be affected. Large lattice mismatches produce high-order commensurate phases in monomer films [7]. Chains tend to lock in glassy phases, and only crystallize for very large  $e^{wf}$  and  $d$  close to the equilibrium monomer spacing along chains.

A wall-induced glass transition provides a natural explanation for the dramatic increases in the measured relaxation times and viscosities of ultrathin films [3–5,11]. To study the dynamic response directly, we sheared our films by translating the top wall at a uniform speed  $v$  in the (100) direction and found the mean frictional force per unit area,  $f$ , exerted on the walls. Figure 2 shows the time-averaged viscosity  $\mu=fh/v$  as a function of  $\dot{\gamma}=v/h$ ,  $m_l$ , and  $P_\perp$  for  $n=6$  films.

The viscous response in Fig. 2(a) for films with  $m_l=8$  typifies the measured behavior of melts of linear polymers. At high  $\dot{\gamma}$ , there is substantial shear thinning with the viscosity obeying a power law of the form  $\mu \sim \dot{\gamma}^{-\alpha}$ . For most polymeric fluids,  $0.4 \leq \alpha \leq 0.9$  [17]. Below a characteristic shear rate,  $\dot{\gamma}_c$ , the viscosity saturates to a limiting value  $\mu_0$ . On time scales longer than  $\tau_{\max}=\dot{\gamma}_c^{-1}$  the film behaves like an ideal Newtonian fluid because stress within it has time to relax. In this regime, the nor-

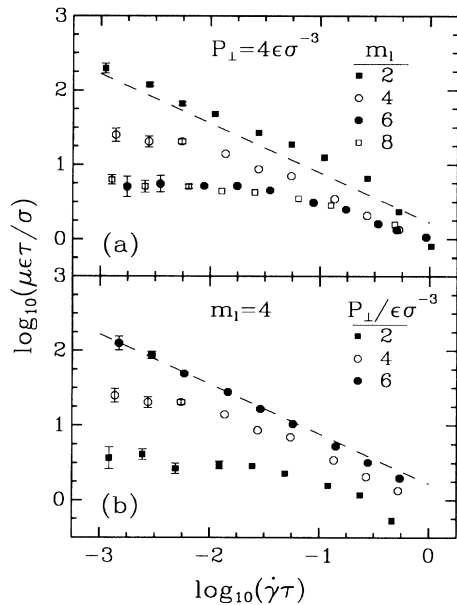


FIG. 2. Variation of  $\mu$  with  $\dot{\gamma}$  as a function of (a)  $m_l$  and (b)  $P_\perp$  in films with  $n=6$ ,  $\epsilon^{wf}=3\epsilon$ ,  $r_c^{wf}=2.2\sigma$ , and  $d=1.0\sigma$ . The dashed lines have slope  $-\frac{2}{3}$ .

mal stress within the film and the wall separation remain constant. For  $\dot{\gamma} > \dot{\gamma}_c$ , the normal stress at fixed  $h$  grows. In simulations at fixed  $P_\perp$ ,  $h$  increases.

Figure 2(a) illustrates how the viscous response of films changes as  $m_l$  decreases. All changes result from confinement since  $P_\perp$  is held fixed. Note that the response at  $m_l=6$  and 8 is identical. This demonstrates that the film exhibits bulklike dynamics down to wall separations of  $\sim 6$  molecular diameters. However, at smaller separations there are dramatic increases in both  $\tau_{max}$  and  $\mu_0$ . By  $m_l=2$ , they have risen by at least 2 orders of magnitude over their bulk values. The relaxation time exceeds the length of our longest simulations ( $\sim 10^6 \Delta t$ ), and the film has a finite yield stress on these time scales. Increases by 3 to 5 orders of magnitude in  $\tau_{max}$  and  $\mu_0$  have been observed in experiments [4,11]. Based on our simulations we attribute them to a confinement-induced glass transition.

The wall separation can also be varied by fixing  $m_l$  and varying  $P_\perp$ . This is particularly relevant to experiments near the glass transition where the extremely slow dynamics inhibit decreases in  $m_l$ . Figures 2(b) and 3 show the dynamic response of  $m_l=4$  and  $m_l=2$  films as a function of  $P_\perp$ . As expected, both  $\tau_{max}$  and  $\mu_0$  are strong functions of  $P_\perp$ . By  $P_\perp=6\epsilon\sigma^{-3}$  in Fig. 2(b) the dynamics in four layer films are too slow to resolve in our simulations. Hu, Carson, and Granick [11] found similar changes in dodecane films. Increasing  $P_\perp$  led to a five-fold increase in both  $\tau_{max}$  and  $\mu_0$  while the number of layers remained fixed. In both their experiments and our simulations the product  $\mu_0\dot{\gamma}_c$  is nearly independent of  $P_\perp$

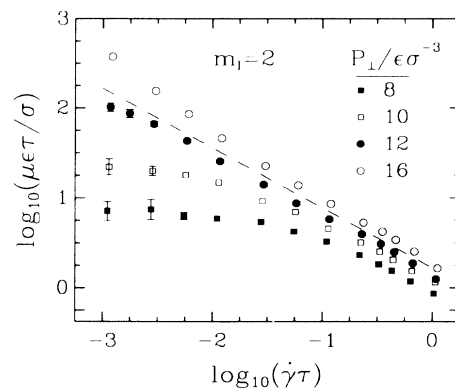


FIG. 3. Variation of  $\mu$  with  $\dot{\gamma}$  as a function of  $P_\perp$  for  $m_l=2$  films with  $n=6$ ,  $\epsilon^{wf}=\epsilon$ ,  $r_c^{wf}=2^{1/6}\sigma$ , and  $d=1.20\sigma$ . The dashed line has slope  $-\frac{2}{3}$ .

and is comparable to the yield stress of a solidlike film.

A striking feature of the non-Newtonian regime in these glassy films ( $\dot{\gamma} > \dot{\gamma}_c$ ) is that the viscosity obeys a power law  $\mu \sim \dot{\gamma}^{-\alpha}$  with  $\alpha \approx \frac{2}{3}$ . The scaling does not depend on many details of the simulations including commensurability between wall and fluid, relative wall orientation, wall stiffness, wall-fluid coupling, or chain length [18]. However, we do find a slight increase in  $\alpha$  as  $P_\perp$  is increased towards the glass transition. The same scaling and variation with  $P_\perp$  has been observed in recent experiments [11]. This is remarkable considering the simplicity of our chain molecules compared to the dodecane, hexadecane, and silicone oil molecules used in the experiments. It suggests that  $\mu \sim \dot{\gamma}^{-2/3}$  may be a universal property of lubricants near a glass transition *under constant normal load* [18]. Simulations at constant  $h$  give similar values of  $\dot{\gamma}_c$ , but the behavior is less universal. The viscosity decreases more slowly with  $\dot{\gamma}$  ( $\alpha \sim \frac{1}{2}$ ) because the film cannot expand to facilitate shear.

Perhaps the most surprising aspect of the power-law response is that the exponent  $\alpha$  does not change when the mechanism of shear changes. Consider, for example, the viscous responses shown in Figs. 2 and 3. While the power laws characterizing the shear-thinning regime are the same, the nature of the strain is fundamentally different. In Fig. 2(b) the strain is uniformly distributed across the film. The film of Fig. 3 behaves like a plug—strain is localized at the wall-fluid interface.

Pluglike flow produces some counterintuitive behavior in thin films. The reason is that the apparent viscosity is no longer a property of the film. Instead, it characterizes the dynamics at the weak wall/film interface. Among other things, this means that  $\dot{\gamma}_c^{-1}$  is not necessarily the largest relaxation time *within* the film. In fact, we found that the films in Fig. 3 were able to maintain stress over a period much longer than  $\dot{\gamma}_c^{-1}$ . We also observed stick-slip motion in these systems at  $\dot{\gamma} < \dot{\gamma}_c$ . In contrast, stress in the films of Fig. 2(a) relaxed to zero with a charac-

teristic time constant of  $\dot{\gamma}_c^{-1}$ , and there was no evidence of stick-slip motion for  $\dot{\gamma} < \dot{\gamma}_c$ . We also found that the apparent viscosity of pluglike films was independent of chain length, while the bulk value of  $\mu_0$  increased rapidly with chain length.

Pluglike flow is most readily observed when  $h$  is much less than the radius of gyration of a free chain. In this limit, each chain occupies a compact region spanning the distance between walls. This structure reflects the large entropic cost for alignment into a single layer or for sharing a region of space with another molecule [19]. Since any velocity gradient tends to stretch the chains, this topology greatly inhibits flow within the film. We found that shear only extended throughout thin films when the range and strength of the wall-fluid coupling were increased so that it could compete with the multiple interactions between chains (Fig. 2).

The entropic constraints become less important as the walls move apart. As they do, the fraction of the strain which occurs within the film increases. Peculiar behavior may result, such as an *increase* in the *effective* viscosity with increasing film thickness. This behavior has been observed in experiments [4], but seems paradoxical since the film is changing from a glass to a fluid. The explanation is that the apparent viscosity measures the total dissipation at the wall/film interface and within the film. As  $h$  increases, there is more strain and dissipation within the film, precisely because its actual viscosity decreases.

The results presented here provide natural explanations for much of the rich behavior observed in molecularly thin films. They suggest that the long relaxation times and power-law decrease in viscosity result from a wall-induced glass transition. While our simulations probe much shorter time scales ( $\sim 1$  ns) than experiment, they indicate that the scaling of the viscosity remains unchanged as the value of  $\tau_{\max}$  increases towards the experimental range. Studies of bulk glasses also reveal that the nature of the dynamics does not change as the characteristic time scale diverges.

From a theoretical standpoint, the most important outstanding issue is what determines the value of  $\alpha$ . A complete description may be complicated by the fact that  $\alpha$  depends on whether the film is allowed to expand. To obtain the value of  $\frac{2}{3}$  one must understand the dependence of both the shear *and* the normal stress on  $\dot{\gamma}$ .

We thank S. Granick, J. N. Israelachvili, and P. M. McGuiggan for sharing their thoughts and data with us.

M.O.R. acknowledges support from National Science Foundation Grant No. DMR-9110004 and the Pittsburgh Superconducting Center, and the hospitality of the Theoretical Physics Institute at the University of Minnesota.

- 
- [1] R. G. Horn and J. N. Israelachvili, *J. Chem. Phys.* **75**, 1400 (1981).
  - [2] D. Y. C. Chan and R. G. Horn, *J. Chem. Phys.* **83**, 5311 (1985); R. G. Horn, S. J. Hirz, G. Hadziioannou, C. W. Frank, and J. M. Catala, *J. Chem. Phys.* **90**, 6767 (1989).
  - [3] J. N. Israelachvili, P. M. McGuiggan, and A. M. Homola, *Science* **240**, 189 (1988).
  - [4] J. Van Alsten and S. Granick, *Phys. Rev. Lett.* **61**, 2570 (1988); *Macromolecules* **23**, 4856 (1990).
  - [5] M. L. Gee, P. M. McGuiggan, J. N. Israelachvili, and A. M. Homola, *J. Chem. Phys.* **93**, 1895 (1990).
  - [6] J. Magda, M. Tirrell, and H. T. Davis, *J. Chem. Phys.* **83**, 1888 (1985); M. Schoen, J. Cushman, D. Diestler, and C. Rhykerd, *J. Chem. Phys.* **88**, 1394 (1988).
  - [7] P. A. Thompson and M. O. Robbins, *Phys. Rev. A* **41**, 6830 (1990).
  - [8] U. Landman, W. D. Luedtke, and M. W. Ribarsky, *J. Vac. Sci. Technol. A* **7**, 2829 (1989); M. Schoen, C. L. Rhykerd, D. J. Diestler, and J. H. Cushman, *Science* **245**, 1223 (1989).
  - [9] P. A. Thompson and M. O. Robbins, *Science* **250**, 792 (1990); M. O. Robbins and P. A. Thompson, *Science* **253**, 916 (1991).
  - [10] M. Lupkowski and F. van Swol, *J. Chem. Phys.* **95**, 1995 (1991).
  - [11] H-W. Hu, G. A. Carson, and S. Granick, *Phys. Rev. Lett.* **66**, 2758 (1991).
  - [12] K. Kremer and G. S. Grest, *J. Chem. Phys.* **92**, 5057 (1990).
  - [13] H. C. Andersen, *J. Chem. Phys.* **72**, 2384 (1980).
  - [14] S. Toxvaerd, *J. Chem. Phys.* **74**, 1998 (1981).
  - [15] P. A. Thompson and M. O. Robbins, *Phys. World* **3**, 35 (1990).
  - [16] At the equilibrium melting point  $S_{\max}/S_0 \sim 0.6$ ; M. S. Stevens and M. O. Robbins (to be published).
  - [17] H. A. Barnes, J. F. Hutton, and K. Walters, *An Introduction of Rheology* (Elsevier, Amsterdam, 1989).
  - [18] P. A. Thompson, G. S. Grest, and M. O. Robbins (to be published).
  - [19] S. K. Kumar, M. Vacatello, and D. Y. Yoon, *J. Chem. Phys.* **89**, 5206 (1988); A. Yethiraj and C. K. Hall, *J. Chem. Phys.* **91**, 4827 (1989); I. Bitsanis and G. Hadziioannou, *J. Chem. Phys.* **92**, 3827 (1990).